



Chaudhuri, T. K., Patel, M. H., Tiwari, D., & Ghediya, P. R. (2018). Kesterite $\text{Cu}_2\text{ZnSnS}_4$ thin films by drop-on-demand inkjet printing from molecular ink. *Journal of Alloys and Compounds*, 747, 31-37. <https://doi.org/10.1016/j.jallcom.2018.03.028>

Peer reviewed version

License (if available):
CC BY-NC-ND

Link to published version (if available):
[10.1016/j.jallcom.2018.03.028](https://doi.org/10.1016/j.jallcom.2018.03.028)

[Link to publication record in Explore Bristol Research](#)
PDF-document

This is the author accepted manuscript (AAM). The final published version (version of record) is available online via Elsevier at <https://www.sciencedirect.com/science/article/pii/S0925838818308879?via%3Dihub> . Please refer to any applicable terms of use of the publisher.

University of Bristol - Explore Bristol Research

General rights

This document is made available in accordance with publisher policies. Please cite only the published version using the reference above. Full terms of use are available: <http://www.bristol.ac.uk/red/research-policy/pure/user-guides/ebr-terms/>

Kesterite Cu₂ZnSnS₄ thin films by drop-on-demand inkjet printing from molecular ink

Tapas K. Chaudhuri^{a*}, Mitesh H. Patel^a, Devendra Tiwari^b and Prashant R. Ghediya^a

^aK. C. Patel Research and Development Centre
Charotar University of Science and Technology, Changa
Anand District, Gujarat 388421, India

^bSchool of Chemistry, University of Bristol
Cantock's Close, Bristol
United Kingdom BS8 1TS

ABSTRACT

Inkjet printing of kesterite Cu₂ZnSnS₄ (CZTS) thin films on glass from molecular ink is described. CZTS ink consists of copper acetate, zinc acetate, tin chloride and thiourea dissolved in a mixture of ethylene glycol and isopropyl alcohol. The printed precursor films are vacuum dried and thermolysed at 200 °C in air to obtain CZTS films. X-ray diffraction and Raman spectroscopy of films confirm the formation of kesterite CZTS without any secondary phases. The band gap of the films is 1.48 eV as deduced from transmission spectrum using Tauc plot. The films are p-type with hole density and mobility of $2.65 \times 10^{19} \text{ cm}^{-3}$ and $0.3 \text{ cm}^2\text{V}^{-1}\text{s}^{-1}$, respectively. Measurement of electrical conductivity of films in the temperature range from 77 to 300 K show that dominant mechanisms of conduction are Mott-Variable Range Hopping, Nearest Neighbour Hopping and Thermally Activated Band Conduction in the temperature ranges of 77 to 155 K, 180 to 240 K and 250 to 300 K, respectively.

Keywords: Copper tin zinc sulfide, inkjet printing, molecular ink, thin film, electrical properties.

*Corresponding author. E-mail: tkchaudhuri.rnd@gmail.com, Fax: +91 2697 247001,
Phone: +91 2697 248285

1. Introduction

Inkjet printing (IJP) is a direct-write, non-contact and non-vacuum method for deposition of solid thin films [1-6]. In this technique, picolitre drops of a liquid ink are impelled onto a substrate to precisely deposit films in pre-defined pattern. The ejected drops fall until they come in contact with the substrate. The drops spread because of momentum and surface tension and eventually coalesce on the substrate to form a film. Printed solid film is then formed by solvent evaporation. IJP has high material utilization factor and eliminates the need for masks. Printed films are likely to be contamination free because of non-contact deposition. Further, IJP is amenable to large scale roll-to-roll deposition of films with sequential and patterning capabilities. Inkjet materials printing (IIMP) has been successfully used in flexible electronics [4,5], organic solar cells [7], electrically conductive contacts [8], ceramics [9], sensors [3,5] and photodetectors [3,5]. However, the use of IIMP for inorganic solar cells is very few [10-13]. There are only recent reports on IJP CZTSSe solar cells [10], In_2S_3 non-toxic buffer layers [11], CZTS films [12] and CIGSSe solar cells [13].

Wang et al. [11] studied IJP In_2S_3 films as non-toxic Cd-free buffer layer for chalcopyrite thin film solar cells. Lin et al. [13] developed IJP CIGSSe solar cells with 12.3 % conversion efficiency. Further, there are only two reports [10,12] so far on IJP of CZTS films: one using molecular solution ink [10] and the other utilizing nanoparticle suspension ink [12]. Lin et al. [10] were first to fabricate IJP CZTSSe solar cells having a photoconversion efficiency of 6.4 %. CZTS precursor layers were printed on Mo/glass substrates from molecular solution ink prepared by dissolving copper (II) chloride, zinc acetate dihydrate, tin (II) chloride dihydrate, thiourea and sodium fluoride in dimethyl sulfoxide (DMSO) with overnight stirring. The printed precursor layers were preheated at 300 °C in air for 2 min to remove solvent. Later, the films were finally annealed in Se vapour at 560 °C for 20 min to obtain CZTSSe films. In a different approach, Martini et al. [12] described IJP of CZTS films from nanoparticle ink. CZTS nanoparticles of 3-5 nm sizes were continuously synthesized from an aqueous solution of tin (IV) chloride, copper acetate monohydrate, zinc acetate dihydrate, 3-mercapto acetic acid and sodium sulphide in a microwave reactor. Nanoparticles were washed, centrifuged and redispersed in methyl-ethyl-ketone with 10 % (v/v) of 1-dodecan-thiol to form inkjet ink. The ink was then used for printing of CZTS with an inkjet material printer (DMP-2831, Fujifilm Diamatix). The as-printed films were dried for 1 hr. under vacuum at 190 °C and then at 300 °C. The ultimate CZTS films were obtained by annealing in sulphur vapours at 540 °C for 3 hr.

In this paper we report inkjet printing of CZTS films on glass from a simple molecular solution ink. The ink consists of a solution of $(\text{Cu}^+-\text{Zn}^{+2}-\text{Sn}^{+2})$ -thiourea (CZTTU) complex dissolved in a blend of ethylene glycol and isopropanol which can be easily prepared in 20 min. The printed precursor films were first dried at 70 °C in vacuum followed by heating in air at 200 °C. Films thus obtained are kesterite CZTS as confirmed by X-ray diffraction and Raman spectroscopy. Electrical properties of such films have been also investigated in the wide temperature range of 77 to 300 K.

2. Experimental

2.1 Formulation of ink

Molecular solution ink basically consists of a precursor dissolved in a solvent. Chaudhuri et al. [14] showed that precursor of $(\text{Cu}^+-\text{Zn}^{+2}-\text{Sn}^{+2})$ -thiourea (CZTTU) complex yields kesterite CZTS on heating. Precursor solution was prepared by dissolving copper (II) acetate monohydrate (0.1 M), zinc acetate dihydrate (0.05 M), tin (II) chloride (0.05 M) and thiourea (TU, 0.5 M) in methanol and films were prepared by dip-coating. Later, Ghediya et al. [15] also reported doctor-blade coating of CZTS films from a solution of CZTTU complex in ethylene glycol (EG). Hence, CZTTU complex was chosen as the precursor for CZTS films.

Next step was to select appropriate solvent suitable for inkjet printing. The solvent had to satisfy the following criteria: (i) it should dissolve readily all the precursor chemicals mentioned above, (ii) the viscosity should be between 10-12 cPs and (iii) surface tension should be between 28 to 33 dynes/cm. As mentioned above, the precursor chemicals dissolved in both methanol [14] and EG [15]. Hence, a mixture of EG and isopropanol (IP) was used as the solvent. EG-IP mixtures with different proportions were prepared and viscosity and surface tension were measured to tune the fluid properties to the desired values. It was found that a blend of 40 % by volume of EG with 60 % by volume of IP has viscosity and surface tension of 10 cPs and 35 dynes/cm, respectively which was close to the targeted values. Thus, for preparing inkjet printing ink, solvent with 40 % EG and 60 % IP was used.

Inkjet ink was prepared by dissolving copper (II) acetate monohydrate (0.2 M), zinc acetate dihydrate (0.1 M), tin (II) chloride (0.1 M) and thiourea (0.8 M) in EG-IP at room temperature (~300 K). At first, 50 mL of EG-IP was taken in a beaker and stirred continuously by a magnetic stirrer. Copper (II) acetate powder was slowly added to EG. A dark blue suspension was formed which turns into dark blue clear solution on adding a few drops of concentrated hydrochloric acid. Then zinc acetate powder was slowly put into the solution which gradually changes into light green colour. Further addition of tin (II) chloride turns the solution into light yellow.

Finally, thiourea (TU) powder was slowly introduced into the solution which first becomes curdy and then turns colourless as shown in Fig.1. TU reduces Cu(II) to Cu(I) under acidic condition to form colourless $[\text{Cu}(\text{TU})_3]^+$ complex [16]. TU also forms complexes with Zn^{++} and Sn^{++} as $[\text{Zn}(\text{TU})_2]^{++}$ and $[\text{Sn}(\text{TU})]^{++}$, respectively. Finally, a colourless complex $[\text{CuZnSn}(\text{TU})_n]^{m+}$ is formed in the EG-IP solvent which is the desired CZTS molecular solution ink. Total time taken for preparing CZTS ink is about 20 min. The ink has been found to be very stable for more than a year. Here, EG not only acts as a solvent but also as stabiliser for transparent ink. All the chemicals and solvents used in present study are of Analytical Grade supplied by Merck Limited, India.

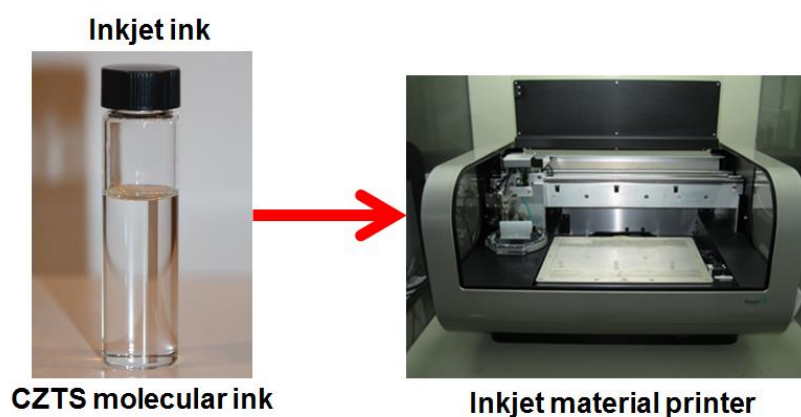


Fig.1 Colourless CZTS molecular ink prepared for inkjet material printing

2.2 Printing of films

The precursor films were printed on glass substrates using an Inkjet Material Printer (DMP2800, Fujifilm Dimatix Inc.). The molecular ink was filtered with a 200 nm filter and injected into a Dimatix printing cartridge (DMC-11610). Scrupulously cleaned glass substrates of sizes 75 mm X 25 mm X 2 and 75 mm X 75 X 2 mm were used for printing. Precursor films of 20 mm X 10 mm patches were printed on the substrates. The printing head has piezo-driven jetting devices with 16 nozzles at 256 μm spacing, each capable of producing drops of 10 pL. The distance between the substrates and printer head was fixed at 1.3 mm. The jetting voltage and dots per inch (DPI) was adjusted to 24 V and 1411, respectively. The films were first dried at 70 °C in vacuum oven (EQ-DZF-6050, MTI Corp.) under a vacuum of 2 torr for 30 min. The solid precursor films were then heated in an oven at 200 °C for 20 min in air for thermolysis to shiny brown CZTS films. Hence, inkjet printing of CZTS films consisted of 3 steps: Inkjet printing of wet precursor films, vacuum drying of prints to get solid precursor films and finally

thermolysing the precursor films to CZTS films by heating at 200 °C in air. In the present study, CZTS films were not subjected any further heat treatment or annealing. Thickness of a single printed film was around 150 nm. For obtaining higher thickness, CZTS films can be printed sequentially one on top of another.

2.3 Characterizations

The composition and crystalline nature of the films were studied by X-ray Diffractometer (Bruker, D2 PHASER). XRD plots were recorded in the 2θ range from 10° to 70° with Ni-filtered $\text{CuK}\alpha$ radiation. The transmittance spectra of the films were measured with a UV-VIS-NIR Spectrophotometer (Shimadzu, UV-3600) in the wavelength range of 300 to 2400 nm. Cross-sectional views of films were observed by Scanning Electron Microscope (SEM, LEO S-440i) attached to the Energy Dispersive Spectroscopy (EDS). The thickness of the films was also estimated from cross-sectional SEM. The vibrational modes of CZTS were studied by Raman Spectrometer (Jobin–Yvon, HR800) with an excitation wavelength of 514 nm. A linearly polarized Ar-ion laser beam with a power of 10 mW was focused into a spot size of 1 μm diameter.

For electrical measurements gap cells (~ 2 mm) were made with graphite paint (Ted Pella) as ohmic contacts. The type of conduction in the films was determined by hot probe method. The electrical conductivity was measured in the temperature ranges of 77 to 300 K by placing the samples in an optical cryostat (Janis VPF-100). The dark current was measured and recorded with a Source/Meter Unit (Keithly 2611) with a DAQ card. During measurements, a constant voltage of 10 V was applied across the contacts of the samples.

3. Results and discussion

Inkjet printing is an upcoming technique used to deposit absorber layers for inorganic thin film solar cells. It is amenable to large scale roll-to-roll printing and patterning for solar cells. This provides a low-cost advantage over conventional fabrication process that involves sequential deposition and patterning. Inkjet printing also has very high materials utilization compared to spin coating and screen printing. Due to this, organic solar cells and other optoelectronic devices such as, light emitting diode and dielectric films has been fabricated using inkjet printing. However, reports on inkjet printing of CZTS films are very few [10,12]. Only, Lin et al. [10] fabricated 6.4 % efficient CZTSSe solar cells based on inkjet-printed absorber layer. The authors deposited CZTS films from solution processed inks in dimethyl sulfoxide

(DMSO). In this paper, inkjet printing of CZTS thin films from transparent ink has been reported. The films were characterized for structural, optical and electrical measurements.

3.1 Inkjet-printed films and characterizations

Fig.2 shows the inkjet-printed CZTS films on glass substrate. Some dots can be found on the final films. This may arise during heating. The films are made up of only a single precursor

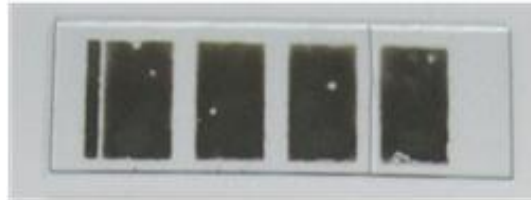


Fig.2 Inkjet-printed CZTS thin films on glass

layer resulting in thickness of 150 nm. Higher thickness can be achieved using layer-by-layer deposition. Chaudhuri et al. [14] proved that single precursor layer of CZTS prepared in methanol resulted in 90 nm. However, it was found that same precursor in EG gives higher thickness.

X-ray diffractogram (XRD) of a typical inkjet-printed CZTS film is shown in Fig.3. There are lines superimposed on background hump because of glass substrate. The XRD lines are identified to be of kesterite CZTS (JCPDS File 26-0575) only due to reflections from (112),

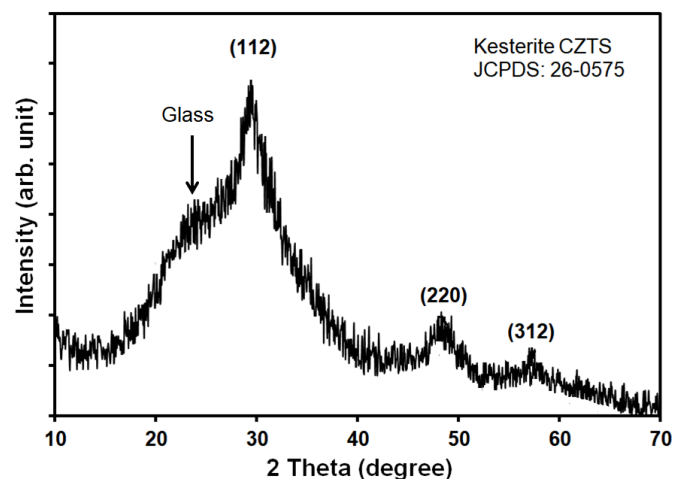


Fig.3 X-ray diffractogram of inkjet-printed CZTS film on glass

(200) and (312) planes. The lines are also broad suggesting that the films are nanocrystalline. The average crystallite size deduced from the Scherrer relation is found to be ~ 10 nm. Similar

results were reported by Chaudhuri and Tiwari [14] for the CZTS films prepared from methanolic ink.

Theoretical and experimental results showed that thermodynamic equilibrium single-phase CZTS is expected to exist only in a narrow region of the pseudo-ternary Cu_2S - ZnS - SnS_2 phase diagram. The narrow phase stability makes defects and secondary phase easy to form during the deposition processes. A slight deviation from the optimal growth conditions (1-2 %) will result in the formation of secondary phases, including, ZnS , Cu_2SnS_3 (CTS), SnS , SnS_2 and CuS . Hence, to confirm the stoichiometry of CZTS, Energy Dispersive Spectroscopy (EDS) was performed. EDS results of printed CZTS films show the presence of Cu, Zn, Sn, S as the major elements. The $[\text{Cu}]/([\text{Zn}]+[\text{Sn}])$ and $[\text{Zn}]/[\text{Sn}]$ ratios are determined to be 0.83 and 1.12, respectively, revealing Cu-poor and Zn-rich stoichiometry [10,12,15]. CZTS solar cells with such compositions have yielded the best efficiency.

There are no extra XRD lines due to any secondary phases, such as, ZnS , Cu_2S , Cu_2SnS_3 (CTS), etc. have been observed. However, crystal structure of CZTS, CTS and ZnS are identical and hence they cannot be detected solely by XRD. Hence, Raman spectroscopy is required to confirm the pure phase. Fig.4 shows the Raman shift spectrum of a typical inkjet-printed CZTS thin film. The spectrum shows the signature peak at 340 cm^{-1} for kesterite CZTS. There are no other secondary lines due to CuS , ZnS , SnS or Cu_2SnS_3 . The peak at 340 cm^{-1} is due to the A1 vibrational mode, arising from the vibrations of sulphur atoms in CZTS lattice while rest of the atoms remains stationary [17]. Thus, it is confirmed that inkjet printing from molecular solution ink yield pure CZTS films.

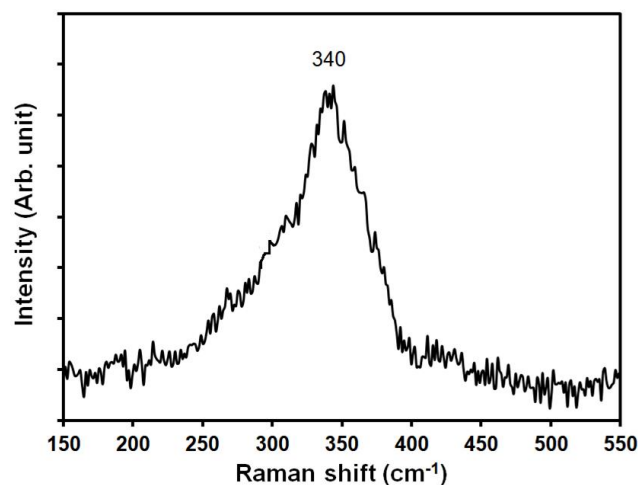


Fig.4 Raman spectrum of inkjet-printed CZTS thin film indicating kesterite phase

The bandgap of printed CZTS film was determined from transmittance spectrum measured in the wavelength range of 350 to 2400 nm. Fig.5(a) shows the transmittance spectrum of single layer deposited CZTS thin film. It can be seen from the Fig. that the transmittance of the film decreases rapidly below 1000 nm due to absorption by CZTS.

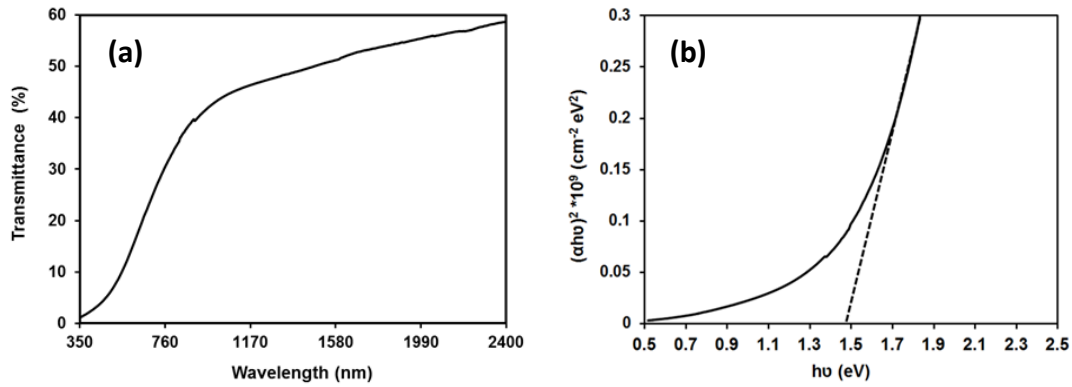


Fig.5 (a) Transmittance spectrum of inkjet-printed CZTS film showing absorption edge and (b) Tauc plot of film indicating direct bandgap of 1.48 eV

The transmittance data was used to calculate the absorption coefficient (α) using Eq. (1):

$$\alpha = \frac{1}{d} \ln \frac{1}{T} \quad \dots\dots\dots(1)$$

where,

d is the thickness and

T is the transmittance of the film

Band gap of CZTS film is determined from the Tauc relation [18] for direct band gap semiconductors:

$$\alpha h\nu = A(h\nu - E_g)^{1/2} \quad \dots\dots\dots(2)$$

where,

α is the absorption coefficient

h is Plank's constant

v is the frequency of radiation

A is an appropriate constant

E_g is the band gap (eV)

Fig.5(b) shows the Tauc plot of $(\alpha h\nu)^2$ Vs. $h\nu$ for printed CZTS film. The band gap of the films was deduced by extrapolating linear portion of the plot to zero and found to be 1.48 eV. This is in good agreement with the reported [19] value of 1.5 eV.

The cross-section of a CZTS thin film as viewed by SEM is presented in Fig.6 which reveals that the film is smooth and homogeneous. The existence of porosity has not been observed. This is similar to the CZTS films made from methanolic solution of CZTTU complex [14]. The above results indicate that IJP precursor films yield CZTS film at 200 °C. IJP ink is a molecular solution of CZTTU complex in EG-IP. This is considerably lower than temperatures reported by Lin et al. [10]. Their IJP films were first pre-heated at 300 °C for solvent removal and then heated at 560 °C in Se. Further, synthesis of molecular ink by Lin et al. [10] takes quite long time: overnight soaking of the precursor chemicals in DMSO. In the present investigation preparation of ink takes only 10 min.

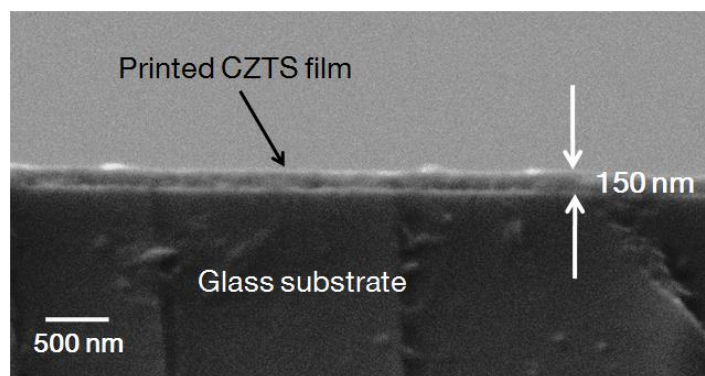


Fig.6 Scanning electron micrograph of the cross-section of a CZTS film inkjet-printed on glass

3.2 Electrical properties

Printed CZTS film was p-type with electrical conductivity (σ) and thermoelectric power (TEP) of 0.5 S/cm and +100 μ V/K, respectively. The hole concentration (p) and mobility (μ) of the film was $2.65 \times 10^{19} \text{ cm}^{-3}$ and $0.3 \text{ cm}^2\text{V}^{-1}\text{s}^{-1}$, respectively as deduced from TEP and σ . This high value of p is probably due to impurities in precursor chemicals and defects. Similar values were also observed for CZTS films dip-coated [14] and doctor-bladed [15] from molecular inks made from same precursor chemicals.

The temperature variation of electrical conductivity (TVEC) of a typical printed CZTS film from 77 to 300 K is shown in Fig. 7 as represented by the plot of $\ln(\sigma)$ vs. $1/T$. In general, the conductivity of film increases with increase in temperature which is characteristic behaviour of a typical semiconductor film. At low temperatures below 125 K (until 77 K), conductivity of the film almost remain constant with temperature. However at higher

temperatures above 200 K, the conductivity of the film increases rapidly. The features of TVEC of a sample depend strongly on the mode of conduction dominant in different temperature ranges. It has been found [15,20,21] that different types of conduction modes take place in CZTS films depending on the temperature range. These include, Efros–Shklovskii variable range hopping (ES-VRH), Mott variable range hopping (M-VRH), nearest neighbour hopping (NNH), thermionic emission over grain boundary barriers (TE over GBB) and thermally activated band conduction (TABC).

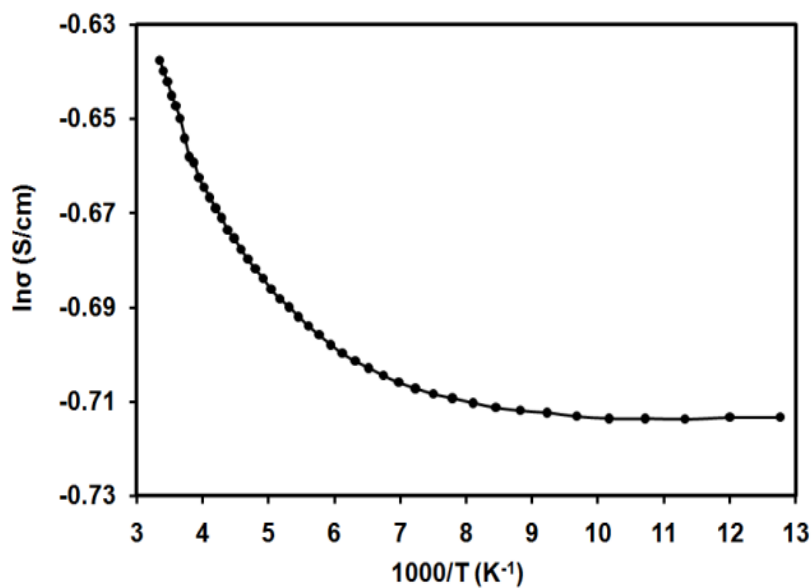


Fig.7 Temperature variation of electrical conductivity of a inkjet-printed CZTS film from 77 to 300 K

In general, hopping conduction in samples occurs below about 180 K through defect states in the band gap. Above about 180 K, polycrystalline CZTS samples show band conduction due to TE over GBB or TABC from defect states. Hence, the data of Fig. 7 was fitted with different models to identify the modes of conduction prevalent in the printed CZTS film.

In the temperature region 77 to 155 K, the plot of $\ln(\sigma)\sqrt{T}$ Vs. $T^{0.25}$ was linear as shown in Fig. 8 which implies that conduction is due to M-VRH. The temperature variation of conductivity of sample under M-VRH is given by

$$\sigma\sqrt{T} = \sigma_{0M} \exp\left(\left(-\frac{T_M}{T}\right)^{\frac{1}{4}}\right) \quad \text{..... (3)}$$

where,

σ_{0M} is the hopping conductivity

T_M is Mott characteristics temperature
 T is the temperature

The hopping energy calculated from the slope of the Eq. (3) is found to be 5 meV. This value is less than 10 meV and $T_0/T \gg 1$ which confirms M-VRH conduction at lower temperatures in these CZTS films. Similar results were reported in [21-24]. Guo et al. [22] have observed that sol-gel derived CZTS films show M-VRH conduction in the temperature range of 40 to 175 K. Conduction by M-VRH from 70 to 170 K was also observed by Anasari et al. [21] for CZTS films prepared by ultrasonic assisted chemical vapour deposition. Hamdi et al. [23] reported M-VRH conduction from 80 to 160 K in CZTS pellets. Ghediya et al. [24] also noticed that conductivity of dip-coated CZTS film in the range 77 to 150 K is because of M-VRH.

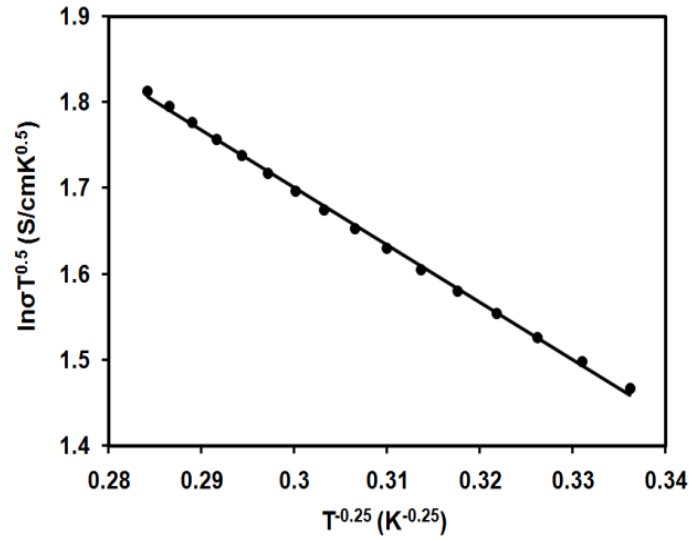


Fig. 8 Plot of $\ln(\sigma)\sqrt{T}$ vs. $T^{-0.25}$ for inkjet-printed CZTS film indicating M-VRH conduction from 77 to 155 K

In the temperature range of 180 to 240 K, the plot of $\ln(\sigma)$ Vs. $1/T$, representing conduction by NNH, was found to be linear as shown in Fig. 9. The variation of conductivity with temperature of samples by NNH is given by

$$\sigma = \sigma_0 \exp\left(-\frac{E_{NNH}}{k_b T}\right) \quad \dots\dots\dots(4)$$

Where,

σ_0 is an appropriate constant
 E_{NNH} is the hopping energy
 k_b is the Boltzmann constant
 T is the temperature

Hence, the conduction of printed CZTS films is dominated by NNH in the temperature range of 180 to 240 K. The hopping energy is deduced to be 17 meV. This in agreement with the results of Ansari et al. [21] who also observed NNH conduction in CZTS films in the temperature range of 170 to 250 K with hopping energy of about 20 - 30 meV.

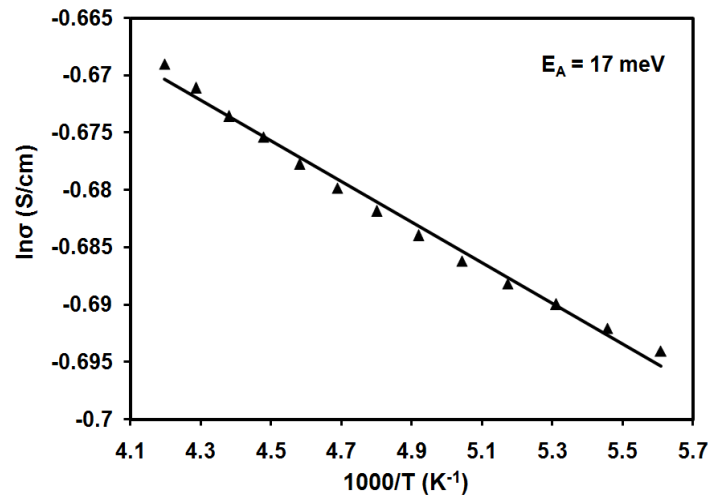


Fig.9 Plot of $\ln(\sigma)$ vs. $1/T$ for inkjet-printed CZTS film suggesting NNH conduction from 180 to 240 K

Finally, analysis of the conductivity data in the temperature range 250 to 300 K show that the plot of $\ln(\sigma)$ Vs. $1/T$ is linear as shown in Fig.10. This reveals that conductivity is thermally activated given by the equation:

$$\sigma = \sigma_0 \exp\left(-\frac{E_a}{k_b T}\right) \quad \dots\dots\dots(5)$$

where,

- σ_0 is a constant and
- E_a is activation energy
- k_b is the Boltzmann constant
- T is the temperature

Thus, electrical conduction in printed CZTS film is due to thermally activated band conduction in the temperature range of 250 to 300 K. The activation energy deduced from slope of the plot is 40 meV. This is probably due to thermal release of holes from defect states copper vacancies (V_{Cu}) situated at 20 meV above valence band and clusters. Furthermore, It can be seen that $\ln(\sigma)$ vs. $1/T$ plot can be fitted with two straight lines: one at higher temperature range (> 200 K) and the other at lower temperatures range (< 200 K), which indicates the presence of NNH

conduction in the lower temperature range. A significant change in activation energy at both the temperature also suggests existing of different transport mode at different temperature.

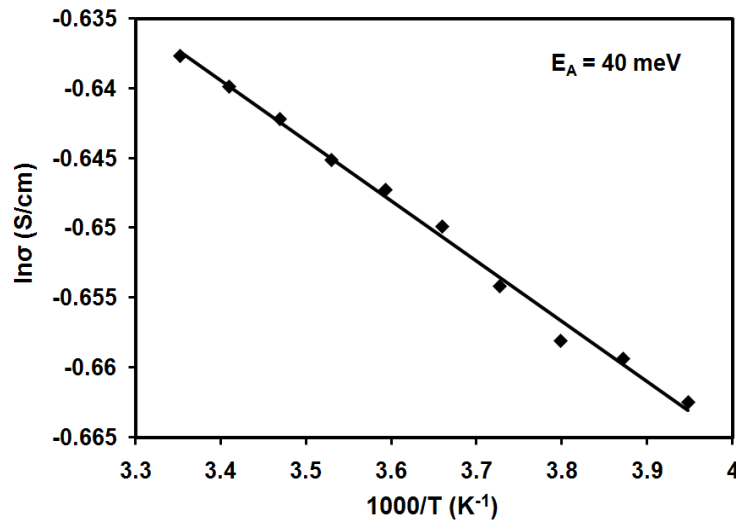


Fig.10 Plot of $\ln(\sigma)$ vs. $1/T$ for inkjet-printed CZTS film from 250 to 300 K

The temperature variation of conductivity (Fig.7) of inkjet-printed CZTS films can be expressed as

$$\sigma = \frac{\sigma_{0M}}{\sqrt{T}} \exp\left(\left(-\frac{T_M}{T}\right)^{\frac{1}{4}}\right) + \sigma_{0N} \exp\left(-\frac{E_{NNH}}{k_b T}\right) + \sigma_0 \exp\left(-\frac{E_a}{k_b T}\right) \quad \dots\dots\dots(6)$$

The first term of the expression is conduction due to M-VRH prevalent from 77 to 155 K ; the second term signifies NNH conduction predominant from 180 to 240 K and third term denotes thermally activated band conduction dominant from 250 to 300 K.

The inkjet-printed CZTS films in the present investigation are basically nanocrystalline. The films are p-type with hole concentration of $\sim 10^{19} \text{ cm}^{-3}$. These films will have dominating intrinsic defects, such as, copper vacancies, V_{Cu} (at 20 meV) and copper on zinc antisites, Cu_{Zn} (120 meV) acting as acceptor levels. High hole concentration in these films implies that density of defect states (situated near the valance band) are also high. Hence, conduction of holes by hopping through these defects states is highly probable. When a printed CZTS film is at low temperatures ($< 250 \text{ K}$), the most of the holes are in the acceptor levels. The thermal energy at these temperatures is insufficient to push the holes to the valence band for conduction. But the energy is sufficient to allow hopping from one level to another in the acceptor levels.

4. Conclusions

Kesterite CZTS films can be inkjet printed on glass from molecular ink consisting of $(\text{Cu}^+-\text{Zn}^{+2}-\text{Sn}^{+2})$ -thiourea complex dissolved in ethylene glycol and isopropanol mixture. The formation of kesterite CZTS were confirmed by XRD and Raman spectroscopy. No other secondary phases were detected. The band gap of inkjet-printed CZTS films is 1.49 eV. The films are p-type with conductivity, hole concentration and mobility of 0.5 S/cm, $2.65 \times 10^{19} \text{ cm}^{-3}$ and $0.3 \text{ cm}^2\text{V}^{-1}\text{s}^{-1}$, respectively. Analysis of temperature dependence electrical conductivity of CZTS films reveals hopping conduction and thermally activated band conduction at lower and higher temperatures, respectively.

Acknowledgements

This work was funded by a grant (DST/TM/SERI/2K10/25) from the Department of Science and Technology, Government of India. The authors are also thankful to the President and Provost of CHARUSAT for support during this work.

References

- [1] E. Tekin, P. J. Smith, U. S. Schubert, Inkjet printing as a deposition and patterning tool for polymers and inorganic particles, *Soft Matter* 4 (2008) 703-713.
- [2] S. E. Habas, H. A. S. Platt, M. F. A. M. van Hest, D. S. Ginley, Low-Cost Inorganic Solar Cells: From Ink to Printed Device, *Chem. Rev.* 110 (2010) 6571-6594.
- [3] M. Singh, H. M. Haverinen, P. Dhagat, G. E. Jabbour, Inkjet Printing-Process and Its Applications, *Adv. Mater.* 22 (2010) 673-685.
- [4] Y. Z. Ping, H. Y. An, B. N. Bin, W. X. Mei, X. Y. Lun, Inkjet printing for flexible electronics: Materials, processes and equipments, *Chinese Sci. Bull.* 55 (2010) 3383-3407.
- [5] J. Perelaer, P. J. Smith, D. Mager, D. Soltman, S. K. Volkman, V. Subramanian, J. G. Korvink, U. S. Schubert, Printed electronics: the challenges involved in printing devices, interconnects, and contacts based on inorganic materials, *J. Mater. Chem.* 20 (2010) 8446-8453.
- [6] B. Derby, Inkjet Printing of Functional and Structural Materials: Fluid Property Requirements, Feature Stability, and Resolution, *Annu. Rev. Mater. Res.* 40 (2010) 395-414.
- [7] T. M. Eggenhuisen, Y. Galagan, A. F. K. V. Biezemans, T. M. W. L. Slaats, W. P. Voorthuijzen, S. Kommeren, S. Shanmugam, J. P. Teunissen, A. Hadipour, W. J. H. Verhees, S. C. Veenstra, M. J. J. Coenen, J. Gilot, R. Andriessen, W. A. Groen, High efficiency, fully inkjet printed organic solar cells with freedom of design, *J. Mater. Chem. A* 3 (2015) 7255-7262.
- [8] B. Derby, Inkjet printing ceramics: From drops to solid, *J. Euro. Ceram. Soc.* 31 (2011) 2543-2550.

- [9] G. Cummins, M. P. Y. Desmulliez, Inkjet printing of conductive materials: a review, *Circuit World* 38 (2012) 193-213.
- [10] X. Lin, J. Kavalakkatt, M. Ch. Lux-Steiner, A. Ennaoui, Inkjet-printed $\text{Cu}_2\text{ZnSn}(\text{S}, \text{Se})_4$ solar cells, *Adv. Sci.* 2 (2015) 1500028-1000033.
- [11] L. Wang, X. Lin, A. Ennaoui, C. Wolf, M. Ch. Lux-Steiner, R. Klenk, Solution-processed In_2S_3 buffer layer for chalcopyrite thin film solar cells, *EPJ Photovolt.* 7 (2016) 70303-70307.
- [12] T. Martini, C. Chubilleau, O. Poncelet, A. Ricaud, A. Blayo, C. Martin, K. Tarasov, Spray and inkjet fabrication of $\text{Cu}_2\text{ZnSnS}_4$ thin films using nanoparticles derived from a continuous-flow microwave-assisted synthesis, *Sol. Energy Mater. Sol. Cells* 144 (2016) 657-663.
- [13] X. Lin, R. Klenk, L. Wang, T. Köhler, J. Albert, S. Fiechter, A. Ennaoui, M. Ch. Lux-Steiner, 11.3% efficiency $\text{Cu}(\text{In}, \text{Ga})(\text{S}, \text{Se})_2$ thin film solar cells via drop-on-demand inkjet printing *Energy Environ. Sci* 9 (2016) 2037-2043.
- [14] T. K. Chaudhuri, D. Tiwari, Earth-abundant non-toxic $\text{Cu}_2\text{ZnSnS}_4$ thin films by direct liquid coating from metal–thiourea precursor solution, *Sol. Energy Mater. Sol. Cells* 101 (2012) 46-50.
- [15] P. R. Ghediya, T. K. Chaudhuri, D. Vankhade, Electrical conduction of CZTS films in dark and under light from molecular solution ink, *J. Alloys Compd.* 685 (2016) 498-506.
- [16] F. H. Jardine, in: H. J. Emeleus and A. G. Sharpe (Eds), *Copper (I) Complexes, Advances in Inorganic Chemistry and Radiochemistry*, Academic Press, New York 17 (1975) 115-163.
- [17] M. Himmrich, H. Haeuseler, Far infrared studies on stannite and wurtzstannite type compounds, *Spectrochim. Acta A* 47 (1991) 933-942.
- [18] J. Tauc, A. J. Menth, States in the gap, *J. Non-Cryst. Solids* 8-10 (1972) 569-585.
- [19] Shiyong Chen, X. G. Gong, Aron Walsh, Su-Huai Wei, Crystal and electronic band structure of $\text{Cu}_2\text{ZnSnX}_4$ ($\text{X}=\text{S}$ and Se) photovoltaic absorbers: First-principles insights, *Appl. Phys. Lett* 94 (2009) 041903-041905.
- [20] V. Kosyak, M.A. Karmarkar, M. A. Scarpulla, Temperature dependent conductivity of polycrystalline $\text{Cu}_2\text{ZnSnS}_4$ thin films, *Appl. Phys. Lett.* 100 (2012) 263903-263907.
- [21] M. Z. Ansari, N. Khare, Thermally activated band conduction and variable range hopping conduction in $\text{Cu}_2\text{ZnSnS}_4$ thin films, *J. Appl. Phys.* 117 (2015) 025706-025712.
- [22] B. L. Guo, Y.H. Chen, X.J. Liu, W.C. Liu, A.D. Li, Optical and electrical properties study of sol-gel derived $\text{Cu}_2\text{ZnSnS}_4$ thin films for solar cells, *AIP Adv.* 4 (2014) 097115-097124.
- [23] M. Hamdi, B. Louati, A. Lafond, C. Guillot-Deudon, B. Chrif, K. Khirouni, M. Gargouri, S. Jobic, F. Hlel, Structural and electrical properties of $\text{Cu}_2\text{Zn}(\text{Sn}_{1-x}\text{Si}_x)\text{S}_4$ ($x = 0, x = 0.5$) materials for photovoltaic applications, *J. Alloys Compd.* 620 (2015) 434-441.
- [24] P. R. Ghediya, T.K. Chaudhuri, J. R. Ray, Effect of light on hopping conduction in kesterite CZTS thin films, *AIP Conf. Proc.* 1728 (2016) 020020-020023.